Title: Episodic activity in a heterogeneous excitatory network, from spiking neurons to mean field

Authors: Boris B. Vladimirski, Joël Tabak, Michael J. O'Donovan, and John Rinzel

Supplementary Material

Methods

Homogeneous network with noise

As described in Introduction, the experimental data exhibit only population synchrony in the active phase, and on a much slower time scale than that of the membrane time constant. To prevent spike-by-spike synchrony caused by phase-locking in the homogeneous network (described in the last section of Results) and make (16) valid, we introduce white current noise into the N-cell model by adding $\sigma\frac{u(t)}{\sqrt{dt}}$ to I_i on the right-hand side of Eq. (4). $\sigma > 0$ is a parameter, $u(t)$ is a random variable uniformly distributed on $(-1;\ 1)$, and dt is the time step. $u(t)$ is chosen independently for each neuron at each time step. With the specified scaling, in the limit $dt \to 0$, the noise term approaches a scaled standard Wiener process with the scaling factor of $\sigma/\sqrt{3}$. σ must be as small as possible to minimize its effect on the response properties of the single cell, but sufficiently large to prevent the synchrony. To quantify the degree of (a)synchrony in the network, we modified the M-measure by Pinsky and Rinzel (1995). The details of this measure are described in Vladimirski (2005). We have found that setting $\sigma = 0.1$ satisfies both requirements for all distributions under consideration, whereas $\sigma = 0.05$ does not.

Modifying the argument by Siegert (1951), Ricciardi (1977), or Rauch et al. (2003), we obtain an analytical expression for the firing rate of a single cell given its bias current I, steady synaptic input g_{syn}, and σ:

$$r(g_{syn},\ I) = \left\{ \tau_{ref} + g_f\sqrt{\pi} \int_{-\sqrt{3}\Theta_{eff}(g_{syn},\,I)/\sigma\sqrt{g_f}}^{\sqrt{3}(1-\Theta_{eff}(g_{syn},\,I))/\sigma\sqrt{g_f}} e^{x^2}(1+\mathrm{erf}(x))\,dx \right\}^{-1} \tag{28}$$

Here we assume that the membrane time constant $\tau = 1$. $g_f = 1/(1+g_{syn})$, $\Theta_{eff}(g_{syn},\ I) = (I + g_{syn}V_{syn})/(1+g_{syn})$ [cf. (9)], and the error function $\mathrm{erf}(x) = \int_0^x e^{-y^2}\,dy$. For $x \ll 0$, i.e., away from the rheobase of the neuron without noise, the integrand is approximately $-1/(\sqrt{\pi}x)$, and we recover expression (8) for the interspike interval of the leaky integrate-and-fire neuron without noise. The noise only affects the firing rate near the pure (no noise) integrate-and-fire firing threshold, where random fluctuations of the membrane potential sometimes bring it above the threshold (Fig. 12). This smoothes out the mean (over time) firing rate curve near the rheobase, though it remains steep, a property of the integrate-and-fire neuron even with noise. Above the pure integrate-and-fire firing threshold, the zero-mean noise whose variance is small over a typical interspike interval, contributes very little to the cell's mean firing rate (Fig. 12).

Mean-field description

In Results, we derived a reduced model of mean-field type [summarized in (14)] to gain insight into episodic rhythmogenesis in the N-cell model. Here we describe how to solve Eq. (14).

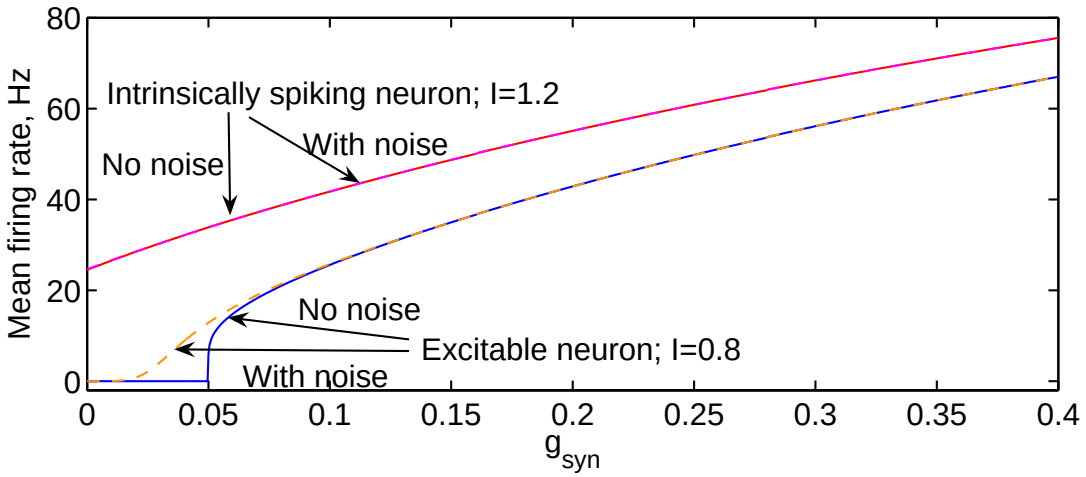

Figure 12: Single-cell firing rate vs. steady synaptic input for the leaky integrate-and-fire neuron with and without noise. The rates are averaged in time and computed analytically using Eq. (28). The noise smoothes out the mean firing rate near the rheobase but has no other appreciable effect.

The use of Eq. (14) or its corollaries requires the computation of the integral on the right-hand side and the subsequent solution of Eq. (14) itself. The integral cannot be computed in elementary functions and thus needs to be evaluated numerically. Additionally, the integral is highly nonlinear in g_{syn}. Therefore, we can only solve (14) numerically in general, incurring approximation errors produced by the mathematical algorithms plus round-off errors caused by implementing those algorithms on a digital computer. Both kinds of errors must be considered and bounded carefully. In analyzing these errors, we assume a digital computer conforming to the IEEE double precision arithmetic (Trefethen and Bau, 1997, pp. 97–100, or Overton, 2001, for a deeper and more extensive exposition), which is an industry standard employed by virtually any machine manufactured in the past 10 years.

The accuracy $\epsilon_{g_{syn}}$ to which the self-consistent value of g_{syn} is computed must be sufficiently fine to ensure that the integral describing the network's input-output relationship [Eq. (14) and Fig. 6(a)] is accurate enough ($\epsilon_{g_{syn}} = 0.01$ is quite sufficient). We use $\epsilon_{g_{syn}} = 10^{-5}$ (for $\tau = 1$) to satisfy the requirements of the dynamical mean-field models based on (14) and (16)–(17).

The accurate numerical evaluation of the integral requires special consideration whose details are given below.

Numerical evaluation of the integral in Eq. (14)

To evaluate the integral numerically, we use composite Simpson's Formula, a commonly used member of the Newton-Cotes family of quadrature formulas (Burden and Faires, 2001, pp. 186–203). Specifically, let a and b arbitrary finite real numbers, $g(x)$ arbitrary scalar function in $C^4[a;\, b]$, n an arbitrary even number, $h = (b-a)/n$ and $x_j = a + jh$ for $j = 0,\, 1,\, \ldots,\, n$.

Then there exists a $\mu \in (a;\ b)$ such that

$$\int_a^b g(x)dx = \frac{h}{3}\left[g(a) + 2\sum_{j=1}^{n/2-1} g(x_{2j}) + 4\sum_{j=1}^{n/2} g(x_{2j-1}) + g(b)\right] - \frac{b-a}{180}h^4 g^{(4)}(\mu) \tag{29}$$

Omitting the last (error) term from the right-hand side, we obtain Simpson's Formula. It is of fourth global order of accuracy, but requires the same number of function evaluations as Trapezoidal or Midpoint formulas that are only second-order.

Now consider the case of a uniform or multimodal distribution of applied currents on $[I_{min};\ I_{max}]$ (the analysis for other distributions is similar and all the important points are covered below). Then, it suffices to consider $g = \hat{q}(g_{syn},\ I)$ from (11), which is in $C^4[a;\ b]$ if we naturally define $\hat{q}(g_{syn},\ I) = 0$ for $r(g_{syn},\ I) = 0$. Using (11) and $p = \beta_q / r(g_{syn},\ I)$ for brevity, we obtain for $r(g_{syn},\ I) > 0$:

$$\frac{d\,\hat{q}(g_{syn},\ I)}{dI} = \frac{d\,\hat{q}(g_{syn},\ I)}{dr}\frac{dr(g_{syn},\ I)}{dI} \tag{30}$$

$$\begin{aligned}\frac{d\,\hat{q}(g_{syn},\ I)}{dr} &= c - \frac{d}{e^{\beta_q/r} - w} + r\frac{d}{\left(e^{\beta_q/r} - w\right)^2}e^{\beta_q/r}\frac{-\beta_q}{r^2} \\ &= c - \frac{d}{e^p - w}\left(1 + \frac{p}{1 - we^{-p}}\right) \qquad (31)\end{aligned}$$

$$e^p \overset{(8)}{=} e^{\beta_q \tau_{ref}}\left(1 + \frac{1}{\Theta_{\mathit{eff}}(g_{syn},\ I) - 1}\right)^{\frac{\beta_q \tau}{1+g_{syn}}} \tag{32}$$

$$\begin{aligned}\frac{dr(g_{syn},\ I)}{dI} &= -r^2\frac{\tau}{1 + g_{syn}}\frac{\Theta_{\mathit{eff}} - 1}{\Theta_{\mathit{eff}}}\left(-\frac{1}{(\Theta_{\mathit{eff}} - 1)^2}\right)\frac{d\Theta_{\mathit{eff}}}{dI} \\ &= \frac{\tau r^2(g_{syn},\ I)}{(1 + g_{syn})^2\,\Theta_{\mathit{eff}}(g_{syn},\ I)\,[\Theta_{\mathit{eff}}(g_{syn},\ I) - 1]} \qquad (33)\end{aligned}$$

Now, $r \downarrow 0 \iff p \to +\infty \iff \Theta_{\mathit{eff}} \downarrow 1 \iff I \downarrow 1 + g_{syn}(1 - V_{syn})$. The dominant term (up to a multiplicative constant) in $d\,\hat{q}(g_{syn},\ I)/dI$ is

$$\frac{r^2(g_{syn},\ I)}{\Theta_{\mathit{eff}}(g_{syn},\ I) - 1}$$

By L'Hôpital's Rule,

$$\lim_{\Theta_{\mathit{eff}} \downarrow 1} \frac{d\,\hat{q}(g_{syn},\ I)}{dI} = +\infty$$

Therefore, if some cells in the population are not firing for a given level of g_{syn}, which is true for the entire duration of the silent phase and at the end of the active phase, this form of $\hat{q}(g_{syn},\ I)$ makes it impossible to obtain a bound on the error induced by the numerical computation of the integral by means of any Newton-Cotes or any other smoothness-based formula. Define

$$I_{min}^a \overset{\text{def}}{=} 1 + g_{syn}(1 - V_{syn}) \tag{34}$$

Then the same is generally (if $f(I^a_{min}) \neq 0$) true for an arbitrary distribution of applied currents:

$$\lim_{I \downarrow I^a_{min}} \frac{d[f(I)\hat{q}(g_{syn},\ I)(I)]}{dI} = \lim_{I \downarrow I^a_{min}} f(I)\frac{d\,\hat{q}(g_{syn},\ I)}{dI} + \underbrace{\lim_{I \downarrow I^a_{min}} \hat{q}(g_{syn},\ I)(I)\frac{df}{dI}}_{0} = +\infty$$

One plausible solution to this problem seems to be to choose a small δI and use

$$\int_{I_{min}}^{I_{max}} \hat{q}(g_{syn},\ I)(I)\,dI = \int_{I^a_{min}}^{I_{max}} \hat{q}(g_{syn},\ I)(I)\,dI \approx \int_{I^a_{min}+\delta I}^{I_{max}} \hat{q}(g_{syn},\ I)(I)\,dI \tag{35}$$

The error in this approximation is

$$\int_{I^a_{min}}^{I^a_{min}+\delta I} \hat{q}(g_{syn},\ I)(I)\,dI \overset{0 \leq \hat{q}(g_{syn},\ I) \leq 1}{\leq} \delta I \tag{36}$$

Nothing can be done to improve this estimate since all the derivatives become infinite at the left endpoint.

Outside $[I^a_{min};\ I^a_{min}+\delta I]$, using the Chain Rule, (30), and (33), we can compute the dominant term in the m^{th} derivative of $\hat{q}(g_{syn},\ I)$ and conclude that it is

$$\mathcal{O}\left[(\Theta_{eff}(g_{syn},\ I) - 1)^{-m}\right] = \mathcal{O}\left[\left(\frac{\delta I}{1+g_{syn}}\right)^{-m}\right] \geq \mathcal{O}\left(\delta I^{-m}\right) \tag{37}$$

Hence, a Newton-Cotes formula of m^{th} global order must be used with $h \leq \mathcal{O}(\delta I^{1+1/m})$ to guarantee accuracy not worse than $\mathcal{O}(\delta I)$. For a reasonable accuracy of 10^{-5}, even with adaptive step control, hundreds of thousands of $\hat{q}(g_{syn},\ I)$-evaluations would be required just to compute $\int_{I^a_{min}+\delta I}^{I_{max}} \hat{q}(g_{syn},\ I)(I)\,dI$ with composite Simpson's Formula. Numerical solution of (14) would raise this number several times further. The required execution time is too long even for (27) and excessive for applications where g_{syn} changes dynamically.

Furthermore, since all the computations are conducted on a digital computer, let us use the following fundamental properties of floating-point arithmetic (Trefethen and Bau, 1997, p. 99) as the basis of all analysis related to the round-off errors:

$$\tilde{x} = x(1+\epsilon_1) \tag{38}$$

$$x \otimes y = (x \times y)(1+\epsilon_2) \tag{39}$$

Here x and y are arbitrary real numbers, $\tilde{x}$ denotes a floating-point representation of x on a digital computer, $\times$ is any one of the four basic arithmetic operations, and $\otimes$ is the implementation of that operation on the digital computer. Finally, $\epsilon_{1,2}$ are some real numbers such that $|\epsilon_{1,\,2}| \leq \epsilon_{machine}$ with $\epsilon_{machine}$ being a maximum relative precision level. Typically, $\epsilon_{machine} \approx 10^{-16}$.

Then, a careful analysis (whose details are not presented in this paper) demonstrates that $\hat{q}(g_{syn},\ I)$ itself can only be computed to $\mathcal{O}(\epsilon_{machine}/\delta I)$. Computing Simpson's Formula in the presence of round-off errors adds another $\mathcal{O}(\epsilon_{machine}/h)$. This implies that even for infinitesimally small integration step h (and infinitely long execution time), it is impossible to achieve accuracy of better than $\approx 10^{-7}$ to 10^{-8}, but we should stress again that even for more modest (and necessary) accuracy values, the execution time for this direct way of evaluating the integral in (14) is impractical. Hence the need for a different approach described in the next section.

Integral transformation

Let $I^\star_{min} = \max(I_{min},\ I^a_{min})$. Then

$$\int_{I_{min}}^{I_{max}} f(I)\hat{q}(g_{syn},\ I)dI = \int_{I^\star_{min}}^{I_{max}} f(I)\hat{q}(g_{syn},\ I)dI \tag{40}$$

To compute $\int_{I^\star_{min}}^{I_{max}} f(I)\hat{q}(g_{syn},\ I)(I)dI$, consider the change of variables

$$x = T(g_{syn},\ I) \tag{41}$$

This change of variables transforms the integral into that with respect to interspike intervals rather than bias currents themselves. Therefore, if the singularity exists ($I^\star_{min} = I^a_{min}$ in the silent phase), it is removed from the integrand and placed into the upper integration limit of $x^\star = +\infty$. Now let

$$x^\star = T(g_{syn},\ I^\star_{min}) \tag{42}$$

$$x_{max} = T(g_{syn},\ I_{max}) \tag{43}$$

In this context, I becomes the inverse function $I(g_{syn},\ x)$ of the transformation (41) with respect to x (g_{syn} is a parameter). Then

$$\int_{I^\star_{min}}^{I_{max}} f(I)\hat{q}(g_{syn},\ I)dI = -\int_{x_{max}}^{x^\star} f(I(g_{syn},\ x))\left(c - \frac{d}{e^{\beta_q x} - w}\right)\frac{dx}{\frac{\partial T(g_{syn},\, I(g_{syn},\, x))}{\partial I}} \tag{44}$$

For integrate-and-fire cells without noise,

$$x = \tau_{ref} + \frac{\tau}{1+g_{syn}}\log\left(1 + \frac{1}{\Theta_{eff}(g_{syn},\ I) - 1}\right) \tag{45}$$

$$\text{Let } \xi = \frac{(1+g_{syn})(x-\tau_{ref})}{\tau}, \text{ then} \tag{46}$$

$$I(g_{syn},\ x) = \frac{1+g_{syn}}{1-e^{-\xi}} - g_{syn}V_{syn} \tag{47}$$

$$\begin{aligned} dx &= \frac{\tau}{1+g_{syn}} \cdot \frac{\Theta_{eff}(g_{syn},\ I) - 1}{\Theta_{eff}(g_{syn},\ I)} \cdot \frac{-1}{(\Theta_{eff}(g_{syn},\ I) - 1)^2} \cdot \frac{1}{1+g_{syn}} dI \\ &= -\frac{\tau(e^\xi - 1)^2 dI}{(1+g_{syn})^2 e^\xi}; \text{ hence,} \end{aligned} \tag{48}$$

$$dI = -\frac{(1+g_{syn})^2}{\tau(e^\xi + e^{-\xi} - 2)}dx \tag{49}$$

While the integrand is no longer a conceptually transparent temporal activation average $\hat{q}(g_{syn},\ I)$, it is now infinitely smooth, monotone and nicely bounded, as are its much easier computable derivatives. Computing this transformed integral numerically requires cutting off its tail at infinity, i.e., choosing an appropriate finite upper limit. This incurs an error that can be rigorously bounded, as can be the effects of the round-off errors caused by the numerical evaluation of the integrand, both limits, and Simpson's Formula on a digital computer. To reach the same accuracy as above for the direct evaluation of the $\hat{q}(g_{syn},\ I)$-integral, 1% or less of execution time needs to be expended. Furthermore, all the related, though long and technical, analysis is greatly simplified as compared to the direct approach. For a general distribution of applied currents, this transformation can be applied to each problematic interval.

Results

Analytical conditions for the knees of the bifurcation diagram and numerical evidence for the predicted bistability

The values of $\overline{g}_{syn}$ and g_{syn} at the knees can be found analytically by requiring that the tangency condition [Fig. 6(b)] be satisfied in addition to the self-consistency condition (14):

$$\frac{g_{syn}}{\overline{g}_{syn}} = g_{out}(g_{syn}) \tag{50}$$

$$\frac{1}{\overline{g}_{syn}} = \frac{dg_{out}(g_{syn})}{dg_{syn}} \tag{51}$$

This is a system of two nonlinear equations in two unknowns, g_{syn} and $\overline{g}_{syn}$. Since $g_{out}(0) > 0$ (we assume there are intrinsically spiking cells in the network), and $g_{out}(g_{syn})$ is bounded by 1 for every g_{syn} because $\hat{q}(g_{in},\, I) \leq 1$ and $f(I)$ is a probability distribution function, one steady state must always exist. If (51), the condition of tangency, is never satisfied, there are no knees, and so the same number of steady states, i.e., one, exists for every $\overline{g}_{syn}$. This is the case in Fig. 7(b), due to the large γ. Generally, the smaller γ is, the more bistable the network is, whereas large values of γ decrease bistability to the point of elimination. When γ is not too large, the bistability is robust with respect to perturbation of the bias currents.

To determine the stability of the steady states, a differential equation describing the evolution of g_{syn} in fast time is necessary. Let us assume, as in Wilson and Cowan (1972) or *ad hoc* models, that this equation can be written as

$$\tau_{g_{syn}} \dot{g}_{syn} = -g_{syn} + \overline{g}_{syn} g_{out}(g_{syn}) \tag{52}$$

Then we can use linear stability analysis to conclude that the low and high steady states are stable, whereas the intermediate one is unstable. This is fully confirmed by simulation results: L and H are observed (and therefore stable) at the predicted values in the predicted $\overline{g}_{syn}$-ranges, whereas M is never seen, confirming its predicted unstable character.

Additionally, we can demonstrate the existence and instability of M as well as the bistability property by applying pulses of current to switch the network from one steady state to the other. Numerical results from the N-cell model shown in Fig. 13 confirm the stability character of the steady states.

In Fig. 13, the network is initialized to be in the low-activity steady state by setting all synaptic conductances to 0 at time 0, and allowed to equilibrate for the period of time equal in duration to 25 membrane time constants, at which moment the stimulus, a short powerful pulse, is given. I_i are uniformly distributed on (0.1; 1.1) and $\overline{g}_{syn} = 0.62$ [corresponding to the three steady states shown in Fig. 7(a)]. The simulations demonstrate the existence of a fixed threshold in g_{syn} at the level predicted by the intermediate steady state M in Fig. 7(a). If immediately following the stimulus the simulated g_{syn} is close to that threshold level, the time course of g_{syn} stays in a neighborhood of the threshold for a long time. This "hesitation" is fully compatible with being near the boundary of the basins of attraction of the other two steady states. Ultimately, numerical effects move it into one of the basins, and it leaves the threshold neighborhood for the corresponding steady state. The same

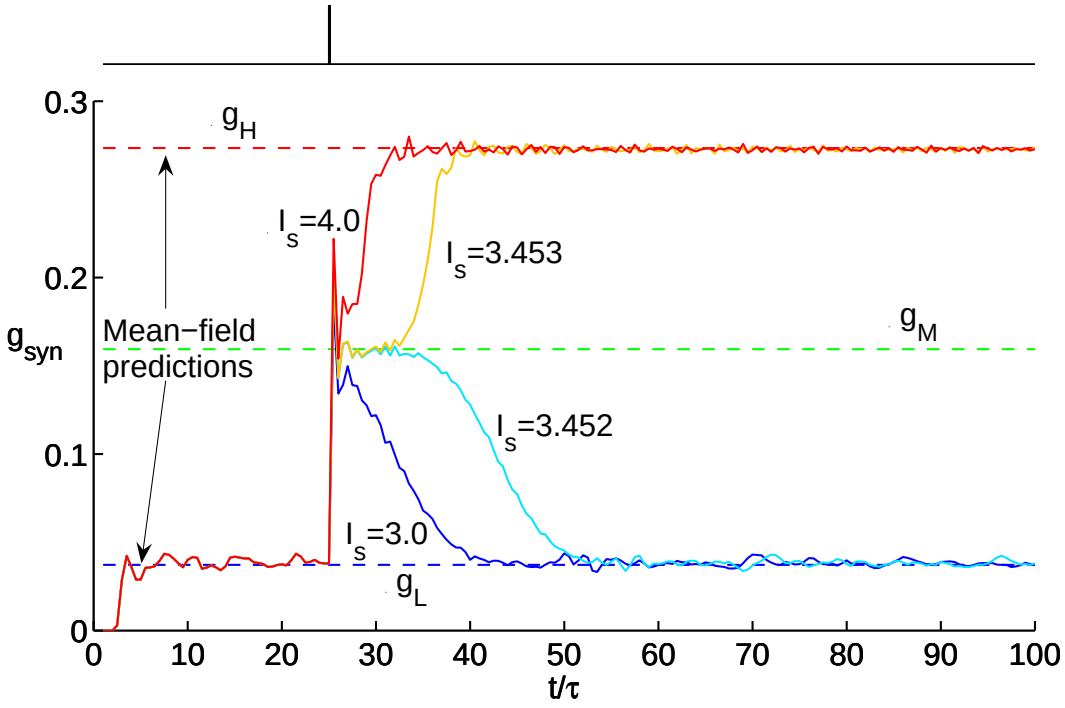

Figure 13: Synaptic drive time courses in response to a uniform stimulus in the nondepressed network. The network is initially in a low-activity steady state and is stimulated, as indicated immediately above the main panel, by a short (2 membrane time constants) powerful current injection that is added to each cell's bias current I_i. The stimulus amplitude I_s is specified next to each time course. The I_i-distribution is the same as in Fig. 7(a) and $\overline{g}_{syn} = 0.62$ [corresponding to three marked steady states, L, M, and H, shown here and in Fig. 7(a)]. The simulation results demonstrate the existence of a fixed threshold in g_{syn} at the predicted level (dashed green line) of the intermediate steady state. This strongly indicates that the intermediate steady state indeed exists at that level and is unstable. The low- and high-activity steady state predictions are also shown as dashed blue and red lines, respectively, and match the simulation results well.

happens if g_{syn} is away from the threshold at the end of the stimulus as well. This strongly indicates that the intermediate steady state exists at the threshold level and is unstable (a saddle). Additionally, the existence and stability of the low- and high-activity steady states is acknowledged. A drop immediately following the stimulus application is caused by transient synchrony when the entire network is recruited to fire almost at the same time.

References

Burden RL, Faires JD (2001) *Numerical Analysis.* Brooks/Cole, Pacific Grove, CA, seventh edition.

Overton ML (2001) *Numerical Computing with IEEE Floating Point Arithmetic.* SIAM, Philadelphia, PA.

Pinsky PF, Rinzel J (1995) Synchrony measures for biological neural networks. *Biological Cybernetics* 73:129–137.

Rauch A, La Camera G, Luscher HR, Senn W, Fusi S (2003) Neocortical pyramidal cells respond as integrate-and-fire neurons to in vivo-like input currents. *Journal of Neurophysiology* 90:1598–1612.

Ricciardi LM (1977) *Diffusion processes and related topics in biology.* Springer-Verlag, Berlin, Germany.

Siegert AJF (1951) On the first passage time probability function. *Physical Review* 81:617–623.

Trefethen LN, Bau D (1997) *Numerical Linear Algebra.* SIAM, Philadelphia, PA.

Vladimirski BB (2005) Modeling and Analysis of Spontaneous Electrical Episodic Activity in the Developing Nervous System by means of a Heterogeneous Excitatory Network of Spiking Neurons with Slow Synaptic Depression and Reduced Mean-field Models Ph.D. diss., New York University, New York, NY.

Wilson HR, Cowan JD (1972) Excitatory and inhibitory interactions in localized populations of model neurons. *Biophysical Journal* 12:1–24.